# High-Resolution Solid-State $^{13}C$ and $^{15}N$ NMR Study on Crystalline Leu- and Met-enkephalins: Distinction of Polymorphs, Backbone Dynamics, and Local Conformational Rearrangements Induced by Dehydration or Freezing of Motions of Bound Solvent Molecules

**Miya Kamihira, Akira Naito,*,† Katsuyuki Nishimura, Satoru Tuzi, and Hazime Saitô*,‡**

*Laboratory of Molecular Biophysics II, Department of Life Science, Himeji Institute of Technology, Harima Science Garden City, Kamigori, Hyogo, Japan 678-1297*

*Received: January 7, 1997; In Final Form: January 13, 1998*

We have recorded $^{13}C$ and $^{15}N$ high-resolution solid-state NMR spectra of Leu-enkephalin trihydrate (**1**, crystallized from aqueous solution), dihydrate (**2**, crystallized from aqueous methanol), $-2H_2O$, 2DMF, X(unspecified solvent) (**3**, crystallized from aqueous *N*,*N*-dimethylformamide (DMF)), and Met-enkephalin·$5.3H_2O$ (**4**, crystallized from aqueous ethanol), at temperatures between 20 and −120 °C, to gain insight into the distinction of these crystalline polymorphs, backbone dynamics, and local conformational rearrangements induced by dehydration or freezing of motions of bound solvent molecules in the crystalline state. Four kinds of crystal forms revealed by X-ray diffraction studies were readily distinguished by $^{13}C$ NMR spectral patterns, and the number of nonequivalent chains in a unit cell was counted by either $^{15}N$ or $^{13}C$ split peaks. NMR signals of two types of independent chains for **1** were resolved at 0 °C but were not distinguishable at ambient temperature owing to either two-site exchange or phase transition. Up to four chains, however, were distinguished for **2**−**4** from the $^{13}C$ and $^{15}N$ NMR splittings of the backbone $C_\alpha$, C═O, N−H, $COO^-$, and/or side-chain Tyr $C_\zeta$ signals. Noticeable spectral changes were induced at the $^{13}C$ NMR signals of the carboxyl group of the terminal Leu residue and Gly $C_\alpha$ by dehydration. It turned out that a distinct conformational change was accompanied with dehydration as manifested from the shortened interatomic distance between the $^{13}C$═O and $^{15}N$−H group, which is four bonds apart. In addition, pronounced spectral changes were noted when motions of bound solvent molecules in the crystals were frozen at lower temperatures. They were interpreted in terms of induced local conformational rearrangement, especially at the N- or C-terminus to which these solvent molecules were coordinated. We further examined the manner of the backbone and side-chain motions by means of the $^{13}C$ and proton spin−lattice relaxation times in the laboratory ($T_1^C$) and rotating frames ($T_{1\rho}^H$), respectively. In particular, the $\beta$-bend structure of crystalline Leu-enkephalin trihydrate turned out to be very flexible in view of $T_1^C$ and $T_{1\rho}^H$ values as compared with the other crystalline forms taking the $\beta$-sheet form. In contrast, there appears no such flexibility in Leu-enkephalin dihydrate despite a claimed similar $\beta$-bend structure as determined by X-ray diffraction. It was also demonstrated that the presence or absence of side-chain motions was conveniently monitored by relative peak intensities of individual residues which were strongly influenced by the manner of local motions interfered with proton decoupling frequency. It was further shown that these molecular motions were also strongly affected by the bound solvent molecules.

## Introduction

Enkephalin is an endogeneous morphine-like substance and is a mixture of Tyr-Gly-Gly-Phe-Met-OH (Met-enkephalin) and Tyr-Gly-Gly-Phe-Leu-OH (Leu-enkephalin). The first four amino acids of the sequence are commonly found in the N-terminus region of endorphin and are essential for the binding to the $\delta$-, $\mu$-, or $\kappa$-receptors consisting of the seven-transmembrane helices.[1−4] In particular, Leu-enkephalin binds to the $\mu$- and $\delta$-receptors, although it prefers the latter.[5] It appears that a specific conformation of enkephalin molecules may play a crucial role for its biological activity. In aqueous media, Leu- and Met-enkephalins are known to be flexible and in equilibrium among several preferred conformations,[6] and the latter contains a type I $\beta$-bend at the residues Gly[3]-Phe[4] in DMSO solution.[7] Leu-enkephalin and its two biologically active analogues, however, adopt a type II′ $\beta$-turn around Gly[3]-Phe[4] and a $\gamma$-turn around Gly[2](or D-Ala[2]) when they are bound to lipid bilayers.[8] In the crystalline state, a number of polymorphs have been revealed by X-ray diffraction studies depending upon solvent composition for crystallization, and these structures can be classified, as a whole, into either the $\beta$-bend[9] or extended forms,[10] although detailed conformations including their torsion angles in the backbone and side-chain orientations differ substantially among the polymorphic structures and also among independent molecules in the unit cells.[9,10] It has been also suggested that the $\beta$-bend conformation binds to the $\mu$-receptor, while the extended form binds to the $\delta$-receptor.[11] This does not always mean, however, that these structures correspond to a biologically active form which is very important to give rise

† E-mail: naito@sci.himeji-tech.ac.jp.
‡ E-mail: saito@sci.himeji-tech.ac.jp.

S1089-5647(97)00106-5 CCC: $15.00 
Published on Web 03/21/1998

to a lead compound for design of a more potent and favorable substance. In principle, such a conformation can be revealed only when enkephalin molecules were studied under the condition of specific binding to the particular receptors in membranes.

To this end, it is expected that REDOR (rotational echo double resonance) NMR,[12] which precisely determines interatomic distances of two labeled nuclei (±0.05 Å) as demonstrated for *N*-acetyl-Pro-Gly-Phe,[13] is expected to be a potentially very suitable means to analyze such biologically active conformations of these ligand molecules bound to the receptors, because crystal samples are not always strictly required to reveal three-dimensional structures by means of NMR. It turned out that the following two points should be clarified in applying REDOR for structure elucidation. First, it is essential to know, in advance, whether these doubly labeled pairs are involved in any sort of molecular motions which modulate dipolar interactions, because such molecular motions, if any, result in errors in the determination of interatomic distances.[14] In such case, these distances should be determined at low temperatures, at which such molecular motions could be frozen. It appears that the possibility of such local motions, if any, depends on the type of crystal form, which is mainly determined by the number of solvent and hydrated water molecules. In addition, it should be pointed out that hydrated water molecules are very easily removed during magic angle spinning unless special care was taken to prevent its evaporation.[15] It was previously shown that the rate of flip-flop motion of the Tyr side chain in Leu-enkephalin is changed by 2 orders of magnitude depending on the extent of hydration, because dehydrated crystal samples gave rise to a different spectral pattern from that of a freshly prepared sample.[15] In this connection, it seems to be very important to explore a new means to know how polymorphic structures of enkephalins could be readily distinguished and how their secondary structures are modified by dehydration or freezing of motions of solvent molecules.

Here, we report a high-resolution solid-state $^{13}C$ and $^{15}N$ NMR study on a variety of Leu- and Met-enkephalin di- and trihydrates placed in a completely sealed rotor to avoid dehydration during magic angle spinning, to distinguish various polymorphs, and to reveal the mechanism of molecular motions in the crystal state. It turned out that dehydration of hydrated crystals results in conformational rearrangements in the backbone, as manifested from reduction of the interatomic distances which are four bonds apart. Pronounced conformational rearrangement was also accompanied by freezing motions of bound solvents at lower temperatures, as viewed from additional splittings or displacements of peaks from the $COO^-$ moiety and Tyr residue, at the C- and N-terminus, respectively.

## Experimental Section

Unlabeled and singly or doubly $^{13}C$-, $^{15}N$-labeled Leu- and Met-enkephalins were synthesized by the solid-phase technique utilizing an Applied Biosystem 431A peptide synthesizer and purified by preparative reversed phase high-pressure liquid chromatography (HPLC) after deprotection. Fmoc-amino acids were purchased from the Peptide Institute, Osaka, Japan. Fmoc isotopically labeled amino acids (99% enriched) were synthesized by the reaction of Fmoc-Osu with the labeled amino acids (from CIL, Andover, MA) following the method of Paquet.[16] These peptides were crystallized from various compositions of solvent systems, after neutralization of saturated aqueous solution with 1 N or 0.5 N KOH solution. The following crystal samples, **1**−**3** of Leu-enkephalin and **4** of Met-enkephalin, were prepared utilizing a variety of solvent systems. Sample **1** (trihydrate) was obtained by slow evaporation of water molecules.[9c,d] Sample **2** (dihydrate) was crystallized by standing Leu-enkephalin in equimolecular solution ($H_2O$ methanol = 1:1) at low temperature (4 °C).[9a,b] Sample **3** (2$H_2O$, 2DMF(*N*,*N*-dimethylformamide), X(unspecified solvent)) was obtained by slow evaporation of solvent molecules from solution in solvent mixtures (DMF $H_2O$ = 2:3).[10a,b] Sample **4** (5.3 $H_2O$) was obtained by standing Met-enkephalin in an equimolecular mixture of ethanol and water at 4 °C.[10c] Specifically $^{13}C$-labeled enkephalins at [1-$^{13}C$]- and [2-$^{13}C$]Gly$^2$ and -Gly$^3$ and [1-$^{13}C$]-Phe$^4$ residues were synthesized after formation of Fmoc of $^{13}C$-labeled amino acid residues. Crystal samples thus obtained were placed in a 5 mm o.d. zirconia rotor tightly sealed with a Teflon cap utilizing Araldyte (Ciba-Geigy) to prevent evaporation of mother liquor.

$^{13}C$ and $^{15}N$ NMR spectra were recorded on a Chemagnetics CMX-400 NMR spectrometer at resonance frequencies of 100.6 and 40.5 MHz, respectively, by the method of cross polarization−magic angle spinning (CP−MAS) with TOSS (total suppression of spinning sidebands).[17] Pulses of 90° used were 4.5−5 $\mu$s, and repetition time was 4 s. Spin−lattice relaxation times were measured by the method of enhancement of the cross polarization with inversion of spin temperature.[18] Cross polarization times ($T_{CH}$) and proton spin−lattice relaxation times in the rotating frame ($T_{1\rho}^H$) were evaluated by a nonlinear least-squares fit of the $^{13}C$ peak intensities $I(t)$ against the contact time $t$ to eq 1, where $I(0)$ denotes the initial peak intensity:[19]

$$I(t) = [I(0)/T_{CH}]\frac{\exp(-t/T_{1\rho}^H) - \exp(-t/T_{CH})}{1/T_{CH} - 1/T_{1\rho}^H} \qquad (1)$$

$^{13}C$ NMR spectra were also recorded after placing a crystal sample in a rotor with a pinhole at the top of a Teflon cap in order to examine how spectral features were changed during the process of dehydration.[13] Low-temperature studies were performed using a cryostat based on a cooled methanol bath (above 0 °C) and liquid nitrogen (below 0 °C) depending upon temperatures.

$^{13}C$ REDOR spectra were recorded to determine $^{13}C\cdots^{15}N$ interatomic distances on the same spectrometer equipped with a triple-resonance probe. Pulse lengths of 90° for the $^{13}C$ and $^{15}N$ nuclei were 5.0 and 7.0 $\mu$s, respectively. A more detailed experimental procedure was described in our previous paper.[13] $^{13}C$ and $^{15}N$ chemical shifts were referred to TMS and ammonium ion ($NH_4NO_3$) through the $^{13}C$ chemical shift of the carboxyl group (176.03 ppm) and $^{15}N$ chemical shifts of Gly in the solid state (11.59 ppm),[20] respectively.

## Results

Figure 1 illustrates $^{13}C$ NMR spectra of a variety of crystal samples recorded at ambient temperature. The signals marked by × are assigned to organic solvents incorporated in the crystals. Rather broad individual single peaks were obtained for **1** despite crystal samples and assigned with reference to the model system,[21] as summarized in Table 1. It turned out, however, that the broadened signals of **1** as compared with **2**−**4** were caused by the coalescence of two signals which are separated by 200−300 Hz at 0 °C, as demonstrated by $^{15}N$ NMR spectra of [$^{15}N$]Leu-labeled **1** at temperatures 25−0 °C (Figure 2). $^{13}C$ or $^{15}N$ NMR spectra of [1-$^{13}C$]- or [$^{15}N$]-labeled crystal samples were also recorded at this temperature, as summarized in Tables 1 and 2. It is noteworthy that two Tyr $C_\zeta$ and/or Met $C_\delta$ were clearly visible as rather sharp signals in **2** and **4**, and

**TABLE 1: $^{13}$C Chemical Shifts of Leu- and Met-Enkephalins in the Crystalline State at Ambient Temperature (ppm from TMS)**

| | COO$^-$ | C=O | | | | $C_\alpha$ | | |
|---|---|---|---|---|---|---|---|---|
| sample | Leu or Met | Tyr[1] | Gly[2] | Gly[3] | Phe[4] | Tyr, Phe, Leu, or Met | Gly[2] | Gly[3] |
| **1** | 178.9 | | 167.1[a] | 166.1[a] | 171.2[b] | 53.9 | 44.3[b] | 44.7[b] |
| | | | 169.8[a] | 168.4[a] | | | | |
| **2** | 178.2 | 167.8[a] | 170.7[a] | 167.1[a] | 170.1[b] | 53.5 | 42.8[b] | 43.1[b] |
| | | 168.1[a] | | | 170.8[b] | 54.2 | 43.9[b] | 44.7[b] |
| **3** | 177.6 | | | | | 54.4 | 41.4[b] | 42.7[b] |
| | 178.7 | | | | | | 42.9[b] | 43.4[b] |
| | 179.4 | | | | | | 44.4[b] | |
| **4** | 176.4 | 167.3 | 167.2[a] | 169.5[a] | 169.8[b] | 54.1 | 43.0[b] | 43.0[b] |
| | | | 168.6[a] | | 171.4[b] | | 44.5[b] | 44.6[b] |

| | Tyr, Phe, Leu, or Met | Tyr | | | | Phe | | Leu or Met | | |
|---|---|---|---|---|---|---|---|---|---|---|
| sample | $C_\beta$ | $C_\gamma$ | $C_\delta$ | $C_\epsilon$ | $C_\zeta$ | $C_\gamma$ | $C_\zeta$ | $C_\gamma$ | $C_\delta$ | solvent |
| **1** | 36.4 | 123.2 | 130.6 | 114.3 | 155.3 | 135.8 | 125.9 | 25.8 | 22.5 | |
| | 39.6 | | | | | | | | 23.7 | |
| **2** | 36.4 | 123.9 | 130.7 | 114.6 | 154.7 | 136.7 | 125.9 | 24.8 | 22.8 | 49.3 |
| | 39.8 | 124.6 | | | 156.0 | | | 26.2 | 23.4 | ($CH_3$) |
| **3** | 38.6 | 125.4 | 130.1 | 115.6 | 156.2 | 137.3 | 127.4 | 24.1 | 19.4 | 31.2 163.1 |
| | 39.4 | 126.2 | 132.6 | | 157.0 | 138.5 | 128.8 | 24.9 | 20.9 | 36.5 (C=O) |
| | 46.3 | | | | 158.3 | | | | 22.2 | ($CH_3$) |
| | 47.0 | | | | | | | | | |
| **4** | 29.8 | 124.4 | 130.4 | 115.0 | 154.9 | 136.3 | 126.6 | 29.8 | 15.7 | 18.0 57.4 |
| | 31.3 | | | | 156.2 | | | 31.3 | 18.3 | ($CH_3$) ($CH_2$) |
| | 34.3 | | | | | | | | | |
| | 35.9 | | | | | | | | | |
| | 40.5 | | | | | | | | | |

[a] From $^{13}$C-labeled samples recorded at 0 °C. [b] From $^{13}$C-labeled samples recorded at ambient temperature.

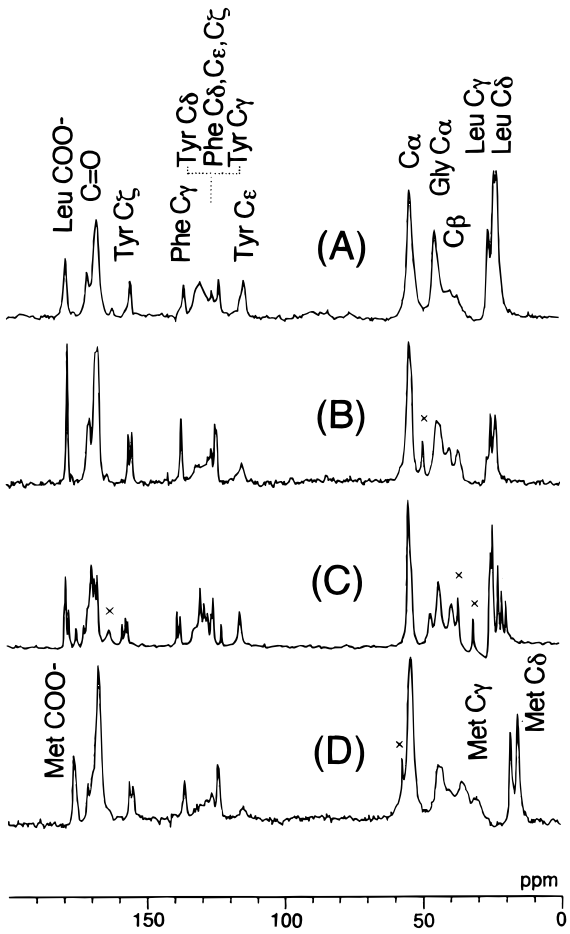


**Figure 1.** $^{13}$C CP−MAS NMR spectra of Leu-enkephalin trihydrate (A; **1**), dihydrate (B; **2**), −$2H_2O$, 2DMF, X(unspecified solvents) (C; **3**), and Met-enkephalin·$5.3H_2O$ (D; **4**) in the crystalline state recorded at 23 °C. Signals marked by × are assigned to the peaks from organic solvents incorporated in the crystals.

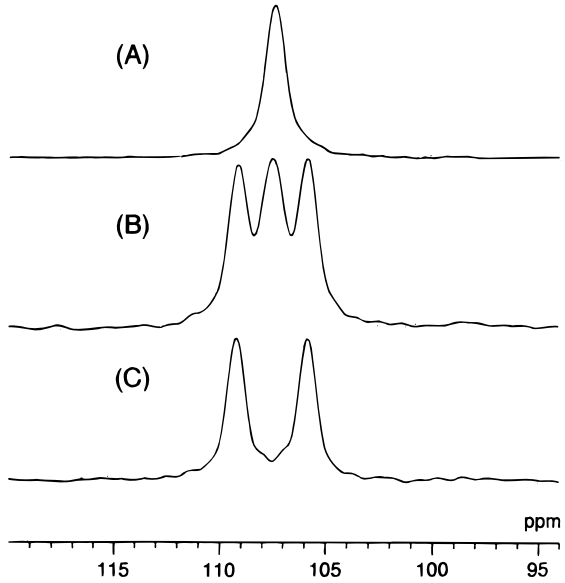


**Figure 2.** $^{15}$N NMR spectra of [$^{15}$N]Leu-enkephalin recorded at temperatures of 25 °C (A), 10 °C (B), and 0 °C (C).

more than three Tyr $C_\zeta$ and Leu carboxyl signals and two Phe $C_\gamma$ signals were resolved for **3**. In addition, the peak intensities of the $C_\delta$ and $C_\epsilon$ signals in Tyr and Phe residues as well as the $C_\beta$ signals of almost all the residues were significantly suppressed as compared with those of Tyr $C_\gamma$ and $C_\zeta$ and Phe $C_\gamma$.

Figure 3 illustrates how $^{13}$C NMR spectra of **2** were changed when water or methanol molecules were gradually removed with the lapse of time through a pinhole at the cap of the rotor under the stream of compressed superdried air. It appears that the single but intense carboxyl signal at the lowermost field was first changed to a doublet at the early stage (within the first 30 min), concomitant with partial disappearance of the methyl signal from bound methanol. A part of the Leu COO$^-$ $^{13}$C NMR signal was then shifted upfield from 178.9 to 175.2 ppm

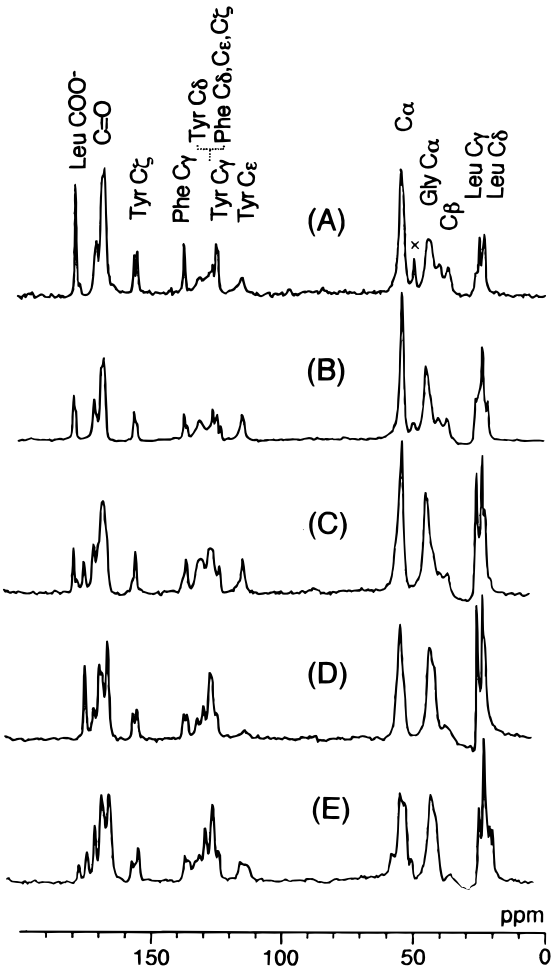


**Figure 3.** Variation of $^{13}C$ CP−MAS NMR spectra of Leu-enkephalin dihydrate (**2**) during the time course of dehydration through a pinhole from the top of a Teflon cap, recorded at 23 °C: (A) freshly prepared, (B) after 30 min, (C) after 1.4 h, (D) after 18 h, (E) after 38 h.

**TABLE 2: $^{15}N$ Chemical Shifts of Leu- and Met-Enkephalins in the Crystalline State (ppm from $NH^{4+}$ ion)**

| sample | Tyr[1] | Gly[2] | | Gly[3] | Phe[4] | Leu[5] or Met[5] |
|---|---|---|---|---|---|---|
| **1** | 14.6 | | 82.9 | | 94.4 | 107.4 |
| | | | 83.8 | | (91.7[a], 96.4[a]) | (105.9[a], 109.3[a]) |
| **2** | 13.4 | 82.1[a] | | 82.1[a] | 92.7[a] | 104.0[a] |
| | 14.5 | 83.5[a] | | 86.4[a] | 94.2[a] | |
| **3** | 14.1 | | 83.6 | | 98.3 | 103.7 |
| | 15.0 | | 84.6 | | 100.6 | 110.5 |
| | 19.4 | | 86.8 | | | |
| | | | 88.1 | | | |
| | | | 93.5 | | | |
| **4** | 13.7 | 82.7[a] | | 82.7[a] | 92.7[a] | 100.4[a] |
| | | 84.4[a] | | 86.8[a] | 94.2[a] | 104.5[a] |

[a] Obtained from $^{15}N$-labeled samples recorded at 0 °C.

after 1.4 h, together with a notable change in the Tyr $C_\zeta$ and Phe $C_\gamma$ signals. It is also noteworthy that the peak intensities of the initially suppressed signals from the aromatic rings in Tyr and Phe were gradually recovered during the course of dehydration from the crystal. The intensities of Tyr $C_\delta$ and $C_\epsilon$ were again suppressed after 18 h. The spectral patterns of Leu $C_\gamma$ and $C_\delta$ signals were subsequently changed at this stage. Finally after 38 h, the Tyr $C_\epsilon$ signal was split into an unresolved doublet pattern, together with the obvious changes in the peak profile for the Tyr $C_\zeta$. It is noted that the crystal was not yet completely dehydrated as compared with the one previously described.[15]

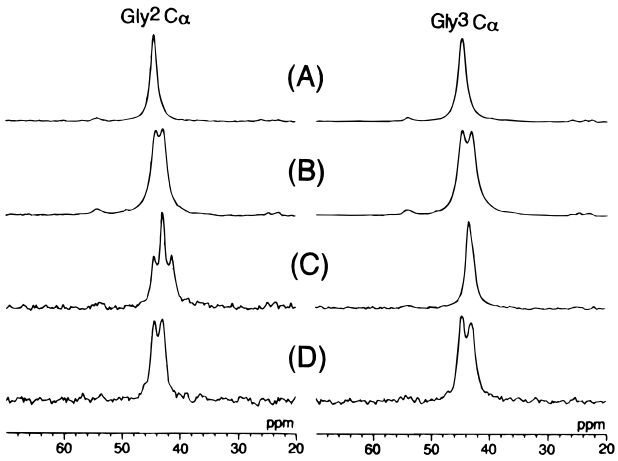


**Figure 4.** $^{13}C$ CP−MAS NMR spectra of [2-$^{13}C$]Gly$^2$- (left) and -Gly$^3$-labeled (right) Leu- and Met-enkephalins, recorded at 23 °C: (A) **1**, (B) **2**, (C) **3**, and (D) **4**.

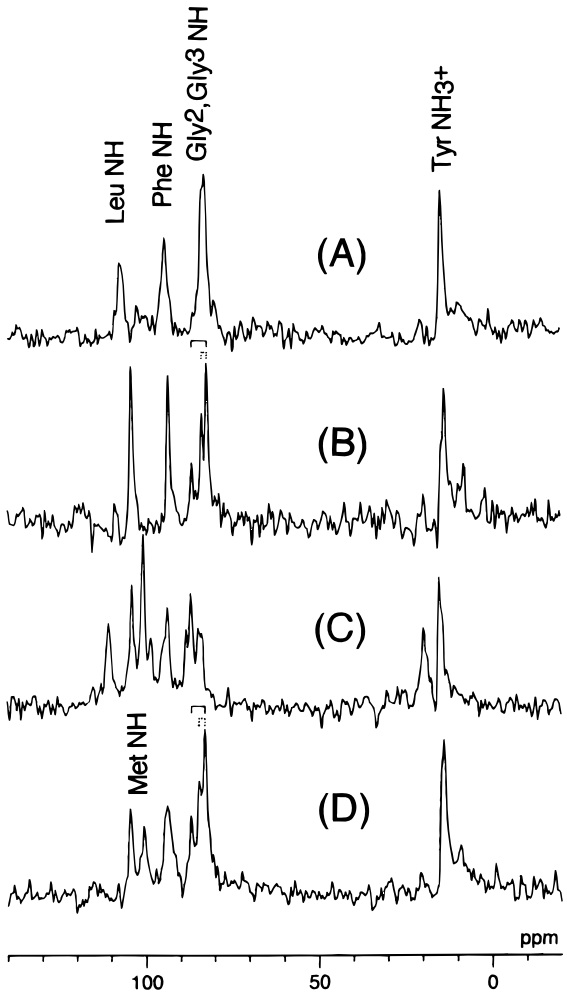


**Figure 5.** $^{15}N$ CP−MAS NMR spectra of crystalline samples **1** (A), **2** (B), **3** (C), and **4** (D) from natural abundance recorded at 23 °C. The peak doublings (solid line for Gly$^3$ and dotted line for Gly$^2$, as confirmed by $^{15}N$-labeled samples, see Table 2) are caused by the presence of two sites in the unit cell.

Figures 4 and 5 illustrate $^{13}C$ CP-MAS NMR spectra of [2-$^{13}C$]Gly$^2$ and -Gly$^3$-labeled and naturally abundant $^{15}N$ CP-MAS NMR spectra of Leu- and Met-enkephalins, respectively, for a variety of crystal forms. The [2-$^{13}C$]Gly $^{13}C$ peaks were straightforwardly assigned by this procedure, as summarized in Table 1. Several $^{15}N$ N−H signals for Gly$^2$, Gly$^3$, Phe, and

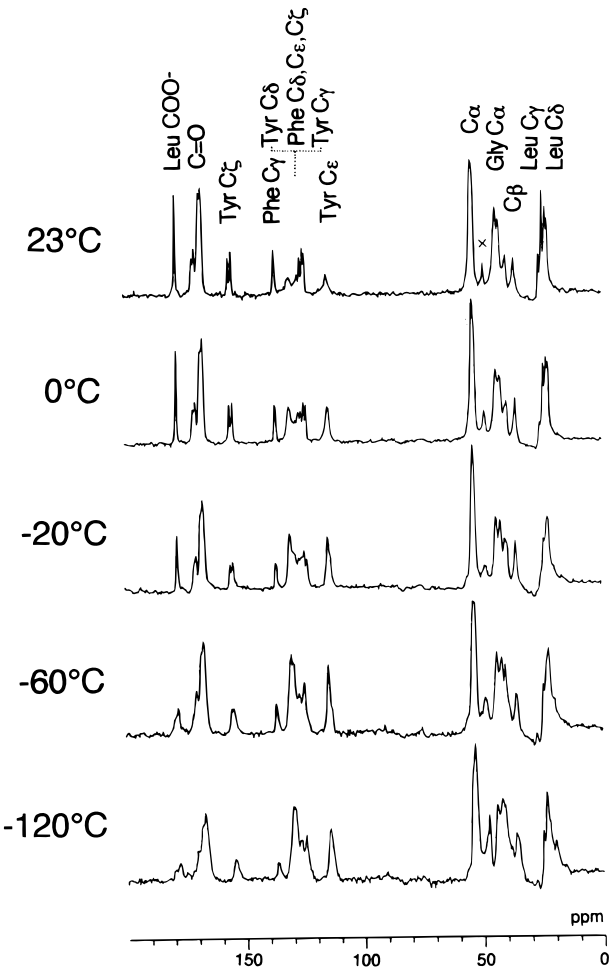


**Figure 6.** Stacked plot of $^{13}C$ CP−MAS NMR spectra of **2** at various temperatures from 23 to −120 °C.

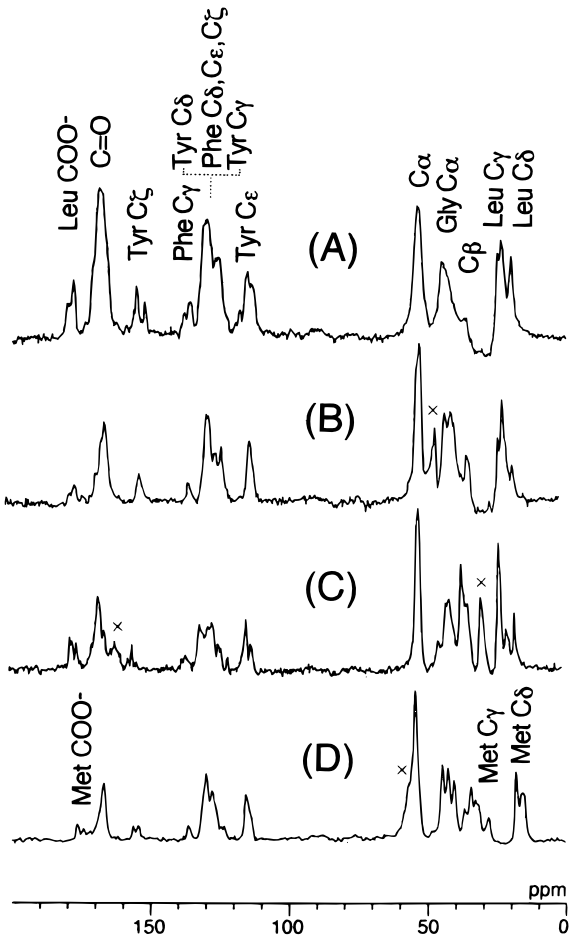


**Figure 7.** $^{13}C$ CP−MAS NMR spectra of **1** (A), **2** (B), **3** (C), and **4** (D) recorded at −100 °C. See the caption of Figure 1.

Leu residues were also assigned by utilizing selectively $^{15}N$-labeled enkephalin sample **1**, **2**, and **4**, as summarized in Table 2, although the assignment of some $^{15}N$ NMR peaks was still tentative in view of the labeled position and with reference to the data in the solution state[22] and also the range of the displacements of peaks due to specific hydrogen bonding.[23] Obviously, the individual $^{13}C$ and $^{15}N$ signals of **1** appeared as singlets, and the latter were particularly assigned to the NH and $NH_3^+$ peaks of the respective amino acid residues. As mentioned already, these singlet $^{13}C$ and $^{15}N$ signals of [1-$^{13}C$]- and [$^{15}N$]-labeled **1** were resolved to yield the doublet signals at 0 °C. The $^{13}C$ and $^{15}N$ signals for the two Gly residues appear as doublets for **2** and **4**, and $^{13}C$ NMR signals for the Met residue appear as doublets for **4**. The manner of the peak splittings appears to be much complicated for **3**: three (1:2:1) peaks were resolved for Gly$^2$, but only a singlet peak was observed for Gly$^3$. In addition, the $^{15}N$ signals should be assigned to four to five peaks, although a precise assignment including the doublet in the Tyr residue is not feasible at the moment.

We recorded $^{13}C$ CP−MAS NMR spectra of **2** at various temperatures between 23 and −120 °C, as illustrated in Figure 6. Further, the $^{13}C$ CP−MAS NMR spectra of these four crystal samples were compared at −100 °C (Figure 7), with reference to those at the ambient temperature (Figure 1). The additional splittings or displacements of peaks from the residues at the N- or C-terminus, $COO^-$, Tyr $C_\zeta$, etc., seem to be characteristic of the low-temperature spectra. It should be emphasized that the maximum proportion of these newly emerging signals apparently at the lowermost field at lower temperature is approximately 1:1 at most even at −140 °C, although spectral change occurred gradually by lowering temperature (Figure 6). No sufficient recovery of the peak intensities was also noted for the $C_\beta$ signals at the temperatures so far studied, however. It is also emphasized that the above-mentioned spectral changes turned out to be completely reversible (spectra not shown).[15]

We measured the $^{13}C$ spin−lattice relaxation times of the laboratory frame ($T_1^C$), $^1H$ spin−lattice relaxation times in the rotating frame ($T_{1\rho}^H$), and cross polarization times ($T_{CH}$) (data not shown) from the stacked plots of varying delay time (spectra not shown), as summarized in Tables 3 and 4, to gain insight into the backbone and side-chain dynamics of these peptides in the crystalline state. Generally, the $^{13}C$ $T_1^C$ values of the carbonyl carbons and the C-terminal Leu $C_\delta$ or Met $C_\delta$ turned out to be 30−40 s and 0.5−1 s, respectively, irrespective of the type of crystalline forms. The $^{13}C$ $T_1^C$ values of the $C_\alpha$, $C_\beta$, and others in **1** are significantly shorter than those of the other crystalline forms **2**−**4**, which exhibit almost the same values. In addition, the $^{13}C$ $T_1^C$ values of methyl groups of the bound solvent molecules, methanol, ethanol, and DMF, are rather long (3−8 s) as compared with those of Leu $C_\delta$ and Met $C_\delta$, in which methyl groups are freely able to undergo $C_3$ rotations without any steric hindrance. The $^{13}C$-resolved proton spin−lattice relaxation times in the rotating frame $T_{1\rho}^H$ are very uniform in sample **3** (3−5 ms) and **4** (2−3 ms), because dominant the spin−diffusion process seems to average out those values. It appears that the $T_{1\rho}^H$ values for the protons in **1** and **2** are rather long (8−20 ms) as compared with **3** and **4**. In particular, the $^{13}C$-resolved $T_{1\rho}^H$ values determined from the

**TABLE 3: $^{13}C$ Spin−Lattice Relaxation Times ($T_1^C$) (s) in the Laboratory Frame of Leu- and Met-enkephalins in the Crystalline State**

| | | | $C_\alpha$ | | | | Tyr | | | | Phe | | | Leu or Met | | |
|---|---|---|---|---|---|---|---|---|---|---|---|---|---|---|---|---|
| sample | $COO^-$ | C=O | | $Gly^2$ | $Gly^3$ | $C_\beta$ | $C_\gamma$ | $C_\delta$ | $C_\epsilon$ | $C_\zeta$ | $C_\gamma$ | $C_{\delta,\epsilon}$ | $C_\zeta$ | $C_\gamma$ | $C_\delta$ | solvent |
| **1** | 13.7 | 35.0 | 8.94 | 6.52[a] | 5.36[a] | 7.00 | 15.8 | 5.50 | 5.09 | 12.1 | 23.3 | 6.83 | 6.06 | 1.01 | 0.83 | |
| **2** | 12.3 | 38.5 | 10.3 | 11.5[a] | 11.4[a] | 11.5 | 28.3 | 18.9 | 14.3 | 22.1 | 36.7 | 17.6 | 12.4 | 1.00 | 0.70 | 8.22 ($CH_3$) |
| **3** | 36.5 | 39.2 | 20.4 | 11.6[a] | 7.07[a] | 11.1 | 21.2 | 14.7 | 12.5 | 37.9 | 26.0 | 6.12 | 9.13 | 1.33 | 0.65 | 3.56 ($CH_3$)<br>33.7 (C=O) |
| **4** | 18.1 | 31.5 | 12.3 | 15.0[a] | 12.5[a] | 14.5 | 29.1 | 14.3 | 14.7 | 22.5 | 22.5 | 34.4 | 14.3 | 7.36 | 2.28 | 3.50 ($CH_3$)<br>8.50 ($CH_2$) |

[a] Determined from $^{13}C$-labeled samples.

**TABLE 4: Proton Spin−Lattice Relaxation Times in the Rotating Frame ($T_{1\rho}^H$) (ms)**

| | | | $C_\alpha$ | | | Tyr | | | Phe | | Leu or Met | | |
|---|---|---|---|---|---|---|---|---|---|---|---|---|---|
| sample | $COO^-$ | C=O | | Gly | $C_\beta$ | $C_\gamma$ | $C_\epsilon$ | $C_\zeta$ | $C_\gamma$ | $C_\zeta$ | $C_\gamma$ | $C_\delta$ | solvent |
| **1** | 40.4 | 25.7 | 17.1 | 16.3 | 16.0 | 31.5 | 19.3 | 64.0 | 31.6 | 21.2 | 20.2 | 23.3 | |
| **2** | 12.8 | 9.00 | 7.84 | 11.5 | 7.81 | 6.37 | 9.01 | 22.8 | 8.23 | 17.6 | 12.0 | 1.00 | 6.98 ($CH_3$) |
| **3** | 3.50 | 3.63 | 4.06 | 4.52 | 4.34 | 4.56 | 4.04 | 5.30 | 3.97 | 5.34 | 4.85 | 5.42 | 20.1 ($CH_3$)<br>3.67 (C=O) |
| **4** | 3.28 | 2.59 | 2.68 | 3.00 | 2.99 | 2.34 | 2.27 | 3.02 | 2.29 | 2.26 | 2.28 | 7.36 | 2.28 ($CH_3$)<br>3.50 ($CH_2$) |

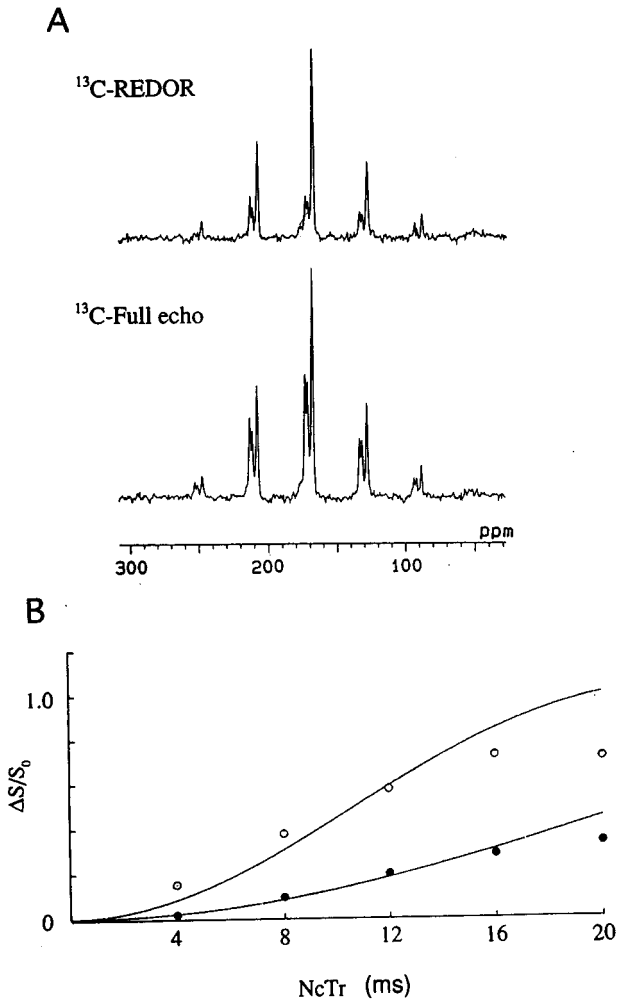


**Figure 8.** $^{13}C$ REDOR (upper trace) and full echo (lower trace) of **2** at $N_cT_r = 12$ ms, recorded at 0 °C (A) and a plot of $\Delta S/S_0$ vs $N_cT_r$ for the dihydrate (closed circles) and partially dehydrated (open circles) components, resepectively. See text for definition.

nonprotonated carbons are 2−3 times as long as those of the protonated carbons (Table 4).

Figure 8A illustrates $^{13}C$ REDOR (upper trace) and full echo (lower trace) of doubly labeled **2** ([1-$^{13}C$]Tyr-Gly-[$^{15}N$]-Phe-Leu dihydrate; the most intense signal) in the presence of partially dehydrated species (the doublet peaks neighbored with the major peak). Obviously, the REDOR effect is more pronounced for the partially dehydrated species resonated as doublets besides the intense signal ascribed to the dihydrate sample. A plot of the normalized echo difference, $\Delta S/S_0$ determined by REDOR experiments vs $N_cT_r$ for the dihydrate (closed circles) and partially dehydrated (open circles) samples, respectively, yielded the interatomic distances of 4.40 and 3.50 Å, respectively (Figure 8B). Here, $S_0$ and $\Delta S$ are the echo amplitudes of full echo and the difference between REDOR and full echo, respectively. $N_c$ and $T_r$ are the number of the rotor cycles and the rotor period, respectively. In a similar way, the distance between $Gly^3$ $^{13}C$=O and Leu $^{15}N$−H was changed from 4.5 to 4.0 Å (spectra not shown). The observed difference in the interatomic distance is significant, although the distance may be prolonged to some extent by correction based on dilution experiments to eliminate the dipolar contribution from labeled nuclei at neighboring molecules.

## Discussion

**$^{13}C$ and $^{15}N$ Spectra Characteristics of Local Conformations of Individual Chains.** As demonstrated, we found that four kinds of crystal samples exhibit different types of $^{13}C$ or $^{15}N$ NMR spectra characteristic of the respective backbone and side-chain conformations and the manner of their crystalline packings (Figure 1). It should be emphasized that the number of split peaks in $^{13}C$ spectra of [2-$^{13}C$]$Gly^2$- and -$Gly^3$-labeled enkephalins, $^{15}N$ spectra of [$^{15}N$]-labeled enkephalins, or those of natural abundance samples gives rise to information as to how many chemically independent chains are present in a given unit cell (Figure 2). It has been demonstrated that $^{15}N$ N−H peaks of peptides are sensitively displaced downfield, in some instances up to 20 ppm,[23] in conformations capable of forming intra- or intermolecular hydrogen bonds. At first glance, it appears that only a single independent chain was present in **1** at ambient temperature, but two independent chains were made visible at 0 °C. This means that the two kinds of independent chains in **1** are present in the unit cell, but they undergo chemical exchange with each other at a rate constant larger than $10^2$ Hz at ambient temperature and/or phase transition at temperatures between 25 and 0 °C. The latter possibility comes from the fact that the singlet and doublet signals instead of a broadened singlet coexist at the intermediate temperature 10 °C (Figure

2). In a similar manner, the presence of two independent chains was confirmed at ambient temperature in **2** and **4**. It is demonstrated that four independent molecular chains are distinguished in the unit cell of **3** by taking into account the splitting of unlabeled Tyr $C_\zeta$ (Figure 1C) and the [2-$^{13}$C]Gly$^2$-labeled peak (Figure 4C) to three peaks (1:2:1 ratio). $^{15}$N peaks were resolved to at least 10 peaks in the range 70−120 ppm (Figure 5C), although 16 peaks due to the presence of four amide nitrogens among four independent chains should be observed. This finding is consistent with the previous data by X-ray diffraction,[9b−d,10a−c] except for **2**. It was shown that the conformation of **2**, initially described as monohydrate, was a $\beta$-bend form consisting of almost four identical chains.[9a] The subsequent X-ray diffraction[9b] study on the same crystal, described later as a dihydrate, shows that there are extra rows of weak spots that are not refined. Instead, we recently revealed a new secondary structure for **2** by means of REDOR experiments that is different from the initial $\beta$-bend form as claimed by X-ray diffraction[9a] but adopts an L-shaped form bent at Gly$^3$.[24]

It is interesting to note that the highest $^{15}$N resonance peaks among the peaks ascribable to the same residues are 82, 92, and 103 ppm, respectively, for Gly$^2$ and Gly$^3$, Phe, and Leu (Met) residues (Table 2). The downfield displacements of the $^{15}$N chemical shifts (2−10 ppm) occurring at the other molecular chain with respect to the above-mentioned peaks are therefore caused by the presence of intra- or intermolecular hydrogen bond(s).[23] It is also interesting to note that the $^{13}$C peak splittings of Leu COO$^-$ of **3** to at least three peaks are caused by the presence of chains whose local conformations are modified at the C-terminal moiety. In a similar way, the splittings of Tyr $C_\zeta$ and/or Phe $C_\gamma$ can be ascribed to the presence of Tyr or Phe residues, in which phenol and aromatic rings interact differently with their surroundings including solvents, and to the different orientations of the side chains. In fact, many previous studies showed that side chains including Tyr, Leu, and Met are disordered,[9a,10a−c] although the Phe side chain was well characterized.[10b] In contrast, it is pointed out in Figure 1 that there exists two types of orientations in the side chain of Phe.

**Local Conformational Rearragements Due to Dehydration or Freezing Motions of Bound Solvent Molecules in the Crystals.** It is now clear that a detailed examination of NMR patterns is very useful to gain insight into how crystal forms are changed during sample handling such as crystallization, filling into the rotor, heating, and cooling, because enkephalin crystals are very unstable unless they are in contact with the mother liquor. Further, they are easily converted to other crystalline forms which are not always well established by X-ray diffraction. As illustrated in Figure 3, the $^{13}$C NMR spectra of **2** seemed to change following the three steps during the time of dehydration. At the beginning, it appears that methanol or other solvent molecules are rather rigidly bound to enkephalin in the crystals, as judged from the observation of $^{13}$C NMR peaks of these solvent molecules by CP−MAS technique and their prolonged relaxation times as compared with those of the liquid state. Nevertheless, they are rather easily removed at an early stage by contact with dry air, although the resulting spectral change in the peptide is minimal at this stage except for the doubling of the Leu COO$^-$ signal. More drastic change of the line shapes, however, was invoked by further dehydration after a lapse of 18 h in the carbonyl and $C_\alpha$ region together with the upfield displacement of the Leu COO$^-$ shift as large as 3.7 ppm.

Such obvious spectroscopic changes can be explained in terms of induced conformational change as visualized by the changes of the interatomic distance caused by partial dehydration (Figure 8). The distance between Tyr $^{13}$C═O and Gly$^3$ $^{15}$N−H, which are four-bonds apart, was reduced from the initial value of 4.4 Å, to 3.5 Å by partial dehydration. A similar explanation can be given to a change from 4.5 to 4.0 Å for the distance between Gly$^3$ $^{13}$C═O and Leu $^{15}$N−H. These findings indicate that partial dehydration of **2** resulted in appreciable conformational rearrangement of the backbone from the initial extended structure to a more folded one. The upfield displacement of the COO$^-$ signal of the C-terminal Leu residue may be due to a breakage of hydrogen bonds to any of the proton aceptors as in intra- or intermolecular hydrogen bonds, bound water molecule(s), etc.

It is now obvious that the hydrated crystal samples are stable only in contact with their mother liquor, and the polar residues at either the N- or C-terminus are surrounded by fluid solvent molecules, as pointed out previously for **3**: many solvent molecules are thus completely disordered and fluid.[10b] It appears that freezing of the motions of such fluid solvent molecules results in local conformational rearrangements, including backbone changes either at the N- or C-terminus and induced side-chain reorientations due to a change in the manner of molecular packing. It is of interest to compare the conformation and dynamics of **2** accompanied by a dehydration process with that of a cooling process. In this connection, it is interesting that the low-temperature spectral patterns at −20 to −40 °C (Figure 6 and spectra not shown) are very close to those of partial dehydration after 30 min (Figure 3). We also found that such freezing of the motions of the bound solvent molecules was detected by the stepwise loss of the central isotropic signals in $^2$H powder patterns of [$^2H_5$]Phe-labeled **2** and **4** as observed at −20, −60, and −120 °C.[25] The peak intensities of the solvent molecules were substantially increased at lower temperatures around −100 °C, because the efficiency of cross polarization of these molecules turned out to be maximal due to the decreased correlation times for internal motions. It is interesting that the variations in the spectral patterns differ substantially probably because of the local conformational rearrangements, concomitant with the above-mentioned stepwise freezing of motions of solvents. The peak separation of Tyr $C_\zeta$ is most pronounced for **1**, probably reflecting the differences in the environments, including the manner of hydrogen bondings of the neighboring hydroxyl groups with water molecules.

It is also noteworthy that the spectral resolution at the $^{13}$C NMR signals of the two Gly signals which are ascribed to either two independent chains or two types (Gly$^2$ and Gly$^3$) of residues was more pronounced for **2**−**4** at −100 °C: the separation of peaks for **2** and **4**, for instance, is 1.3 and 1.4 ppm, respectively, at ambient temperature and is increased to 2.1−2.2 ppm at −100 °C. This significant amount of $^{13}$C chemical shift change should be ascribed to the appreciable change in the backbone conformations for samples **2**−**4** at the Gly residues in view of the conformation-dependent displacements of $^{13}$C NMR peaks.[26] In this connection, it is noteworthy that the initial conformational change occurs at −20 °C. On the contrary, there appears no such spectral change in **1**, consistent with the previous finding by X-ray diffraction study[9e] on the basis of a comparative study at ambient temperature and 100 K.

**Backbone and Side-Chain Dynamics.** It is interesting that the $T_1^C$ values of $C_\alpha$ and $C_\beta$ carbons (5−7 s) in **1** are rather short as compared with those (10−30 s) of **2**−**4** (Table 3), because of probable local small amplitude librational motions

in the peptide backbones on time scales from picoseconds to nanoseconds, as encountered in various peptide systems such as fd coat proteins,[27] collagen,[28] and some peptides containing a Gly-Gly unit including Leu-enkephalin.[29] It is conceivable that such motion could occur more easily in enkephalin consisting of the $\beta$-bend form of loose crystalline packing, but the extended form is more strongly held as a result of dimer formation.[10c,e] In a similar manner, the shorter $T_1^C$ values in the $C_\delta$ and $C_\epsilon$ signals of the aromatic region in Tyr and Phe residues can be accounted for by high-frequency librational motions rather than rapid flip-flop motions, since Phe $C_\zeta$ shows $T_1^C$ values as short as those of $C_\delta$ and $C_\epsilon$. We also detected a high-frequency librational motion of the phenyl rings (correlation time being on the order of $10^{-8}$ s) with small amplitude by means of a line-shape analysis of the $^2H$ NMR signal of [$^2H_5$]-Phe-labeled enkephalins.[25]

The presence of slower motions could be characterized by proton spin−lattice relaxation times in the rotating frame ($T_{1\rho}^H$) and relative peak intensities which are influenced by proton decoupling frequency.[30] As to the former, it is demonstrated in Table 4 that the $^{13}C$-resolved $T_{1\rho}^H$ values for **3** (2−3 ms) and **4** (4−5 ms) are very similar among the protons or carbons not directly attached to protons in the same molecules despite the different environment because these values are averaged out by the dominant spin−diffusion process. This is because these $T_{1\rho}^H$ values are much influenced by either groups undergoing flip-flop motions or $C_3$ rotation of the terminal amino groups with time scale of $10^4-10^5$ Hz. On the contrary, it appears that the $T_{1\rho}^H$ values for **1** and **2** are rather long (16−20 and 6−12 ms, respectively). This means that the spin−diffusion process is not effective for **1** and **2** probably due to the presence of rapid backbone motions as detected by the $T_1^C$ values as described above. It is interesting to note that the $T_{1\rho}^H$ values of the nonprotonated carbons are 2−3 times as long as those from the protonated carbons. This is probably the case in which either the magnetization for the nonprotonated carbons decays with the time constant of $T_{1\rho}^C$ instead of $T_{1\rho}^H$, since neighboring protons behave as isolated spins.

As to the latter, the substantially suppressed peak intensities for $C_\delta$ and $C_\epsilon$ were caused by interference of spin decoupling frequency[30](50 kHz) with the rate of the flip-flop motion ($10^4-10^5$ Hz) of aromatic rings in Tyr and Phe about the $C_\gamma-C_\zeta$ axis. It appears that the $C_\delta$ and $C_\epsilon$ peaks for **1** and **3** are more intense than those for **2** and **4**, while the intensity of **1** increased as the temperature is lowered from ambient temperature. In particular, the minimum intensity for **3** is at 0 °C and recovered at the lower temperatures. Therefore, the rates of the flip-flop motions are different to some extent among the above four types of crystalline samples. It should be emphasized that, from our previous $^{13}C$ NMR studies on anhydrous crystalline enkephalins[14] and model peptides,[31] the Tyr $C_\epsilon$ signals should resonate as distinct doublet signals with a peak separation of up to 4 ppm, as long as the phenol ring of the Tyr residue is static. This is obviously not the case in the crystals studied here, however: only a single line was observed, indicating that the rate constant of flip-flop motions of the Tyr ring about $C_\gamma-C_\zeta$ axis is at least $10^2$ Hz, as viewed from the averaging of these peak separations. The rate constant for the flip-flop motion of Leu-enkephalin dihydrate (crystallized from ethanol) was previously evaluated as $5.6 \times 10^4$ Hz from the line-shape analysis of the $^2H$ powder pattern for the [$^2H_4$]Tyr-labeled sample.[32] This is consistent with the data for all the crystalline samples studied here, estimated from the peak suppression interfered with the decoupling frequency. In a similar manner, the intensity of the $C_\beta$ signal is also substantially suppressed because their motional frequencies might be close to the proton decoupling frequency, which allows severe interference between them.

## Concluding Remarks

We have demonstrated here that $^{13}C$ or $^{15}N$ NMR spectra of Leu- and Met-enkephalins are very sensitively changed to their four kinds of polymorphs, which are grown from solutions consisting of different solvent composition, and this can be considered as a very useful means to distinguish them. It was shown that a local conformational rearrangement due to freezing of motions of solvent molecules was also very conveniently examined in terms of splittigs or displacements of NMR peaks from the residues under consideration. A distinct conformational change due to dehydration was very easily detected by either such splittings or displacement of peaks as well as the change of the interatomic distance between $^{13}C{=}O$ and $^{15}N-H$, which is four-bonds apart. Backbone and side-chain dynamics of these enkephalin molecules occurring at different time scales were also very conveniently examined in terms of peak suppression due to the decoupling frequency interfered with molecular motion, $^{13}C$ spin−lattice relaxation times in the laboratory frame, and proton spin−lattice relaxation times in the rotating frame.

**Acknowledgment.** This work was supported, in part, by Grants-in-Aid for Scientific Research from the Ministry of Education, Science, Sports and Culture of Japan.

## References and Notes

(1) Hughes, J.; Smith, T. W.; Kosterlitz, H. W.; Fothergill, L. A.; Morgan, B. A.; Morris, H. R. *Nature* **1975**, *258*, 577.

(2) Chavkin, C.; Goldstein, A. *Proc. Natl. Acad. Sci. U.S.A.* **1981**, *78*, 6543.

(3) Wolozin, B. L.; Pasternak, G. W. *Proc. Natl. Acad. Sci. U.S.A.* **1981**, *78*, 6181.

(4) Schiller, P. W. *The Peptides, Analysis, Synthesis, Biology*; Udenfriend, S., Meienhofer, J., Eds.; Academic Press: Orlando, 1984; Vol. 6, p 269.

(5) Paterson, S. J.; Robson, L. E.; Kosterlitz, H. W. *The Peptides, Analysis, Synthesis, Biology*; Udenfriend, S., Meienhofer, J., Eds.; Academic Press: Orlando, 1984; Vol. 6, pp 147.

(6) Khaled, M. A.; Urry, D. W.; Bradley, R. J. *J. Chem. Soc., Perkin Trans. 2*, **1979**, 1693.

(7) Stimson, E. R.; Meinwald, Y. C.; Scheraga, H. A. *Biochemistry* **1979**, *18*, 1661.

(8) Milon, A.; Miyazawa, T.; Higashijima, T. *Biochemistry* **1990**, *29*, 65.

(9) (a) Smith, G. D.; Griffin, J. F. *Science* **1977**, *199*, 1214. (b) Blundell, T. L.; Hearn, L.; Tickle, I. J.; Palmer, R. A.; Morgan, B. A.; Smith, G. D.; Griffin, J. F. *Science* **1979**, *205*, 220. (c) Aubry, A.; Birlirakis, N.; Sakarellos-Daitsiotis, M.; Sakarellos, C. *J. Chem. Soc., Chem. Commun.* **1988**, 963. (d) Aubry, A.; Birlirakis, N.; Sakarellos-Daitsiotis, M.; Sakarellos, C.; Marraud, M. *Biopolymers* **1989**, *28*, 27. (e) Wiest, R.; Pichon-Pesme, V.; Benard, M.; Lecomte, C. *J. Phys. Chem.* **1994**, *98*, 1351. (f) Ishida, T.; Kenmotsu, M.; Mino, Y.; Inoue, M.; Fujiwara, T.; Tomita, K.; Kimura, T.; Sakakibara, S. *Biochem. J.* **1984**, *218*, 677.

(10) (a) Camerman, A.; Mastropaolo, D.; Karle, I.; Karle, J.; Camerman, N. *Nature* **1983**, *306*, 447. (b) Karle, I. L.; Karle, J.; Mastropaolo, D.; Camerman, A.; Camerman, N. *Acta Crystallogr.* **1983**, *B39*, 625. (c) Mastropaolo, D.; Camerman, A.; Camerman, N. *Biochem. Biophys. Res. Commun.* **1986**, *134*, 698. (d) Griffin, J. F.; Langs, D. A.; Smith, G. D.; Blundell, T. L.; Tickle, I. J.; Bedarkar, S. *Proc. Natl. Acad. Sci.* **1986**, *83*, 3272. (e) Doi, M.; Tanaka, M.; Ishida, T.; Inoue, M.; Fujiwara, T.; Tomita, K.; Kimura, T.; Sakakibara, S.; Sheldrick, G. M. *J. Biochem.* **1987**, *101*, 485.

(11) (a) Soos, J.; Berzetei, I.; Bajusz, S.; Ronai, A. Z. *Life Sci.* **1980**, *27*, 129. (b) Fournier-Zaluski, M. C.; Gacel, G.; Maigret, B.; Premilat, S.; Roques, B. P *Mol. Pharmacol.* **1981** *20*, 484.

(12) Gullion, T.; Schaefer, J. *J. Magn. Reson.* **1989**, *81*, 196.

(13) (a) Naito, A.; Nishimura, K.; Tuzi, S.; Saitô, H. *Chem. Phys. Lett.* **1994**, *229*, 509. (b) Naito, A.; Nishimura, K.; Kimura, S.; Tuzi, S.; Aida, M.; Yasuoka, N.; Saitô, H. *J. Phys. Chem.* **1996**, *100*, 14995.

(14) Hing, A. W.; Schaefer, J. *Biochemistry* **1993**, *32*, 7593.

(15) Naito, A.; Kamihira, M.; Tuzi, S.; Saitô, H. *J. Phys. Chem.* **1995**, *99* (9), 12041.
(16) Paquet, A. *Can. J. Chem.* **1982**, *60*, 976.
(17) Dixon, W. T. *J. Chem. Phys.* **1982**, *77*, 1800.
(18) Torchia, D. A. *J. Magn. Reson.* **1978**, *30*, 613.
(19) Mehring *High-Resolution Solid State NMR Spectroscopy in Solids*; Springer-Verlag: New York, 1983.
(20) Shoji, A.; Ozaki, T.; Fujito, T.; Deguchi, K.; Ando, S.; Ando, I. *J. Am. Chem. Soc.* **1990**, *112*, 4693.
(21) Howarth, O. W.; Lilley, D. M. J. *Prog. Nucl. Magn. Reson. Spectrosc.* **1978**, *12*, 1.
(22) Nyasse, B.; Grehn, L.; Ragnarsson, U. *J. Chem. Soc., Chem. Commun.* **1994**, 2005.
(23) (a) Witanowski, M.; Webb, G. A. *Nitrogen NMR*; Plenum, London, 1973. (b) Levy, G. C.; Lichter, R. L. *Nitrogen-15 Nuclear Magnetic Resonance Spectroscopy*; John Wiley and Sons: New York, 1979. (c) Saitô, H.; Nukada, K. *J. Am. Chem. Soc.* **1971**, *93*, 1077. (d) Saitô, H.; Tanaka, Y.; Nukada, K. *J. Am. Chem. Soc.* **1971**, *93*, 1077.
(24) Nishimura, K.; Naito, A.; Tuzi, S.; Saitô, H. *Proceedings of 35th Japanese NMR Symposium*, Kyoto, 1996; pp 417−420.
(25) Naito, A.; Kamihira, M.; Tuzi, S.; Saitô, H. *Proceedings of 35th Japanes NMR Symposium*, Kyoto, 1996; pp 120−123.
(26) (a) Saitô, H. *Magn. Reson. Chem.* **1986**, *24*, 835. (b) Saitô, H.; Ando, I. *Annu. Rep. NMR Spectrosc.* **1989**, *21*, 209
(27) Cross, T. A.; Opella, S. J. *J. Mol. Biol.* **1982**, *159*, 543.
(28) Sarkar, S. K.; Sullivan, C. E.; Torchia, D. A. *Biochemistry* **1985**, *24*, 2348.
(29) Naito, A.; Fukutani, A.; Uitdehaag, M.; Tuzi, S.; Saitô, H. *J. Mol. Struct.* **1998**, *441*, 231.
(30) Rothwell, W. P.; Waugh, J. S. *J. Chem. Phys.* **1981**, *74*, 2721.
(31) Saitô, H.; Ishida, M.; Yokoi, M.; Asakura, T. *Macromolecules* **1990**, *23*, 83.
(32) Rice, D. M.; Witterbort, R. J.; Griffin, R. G.; Meirovitch, E.; Stunsibm, E. R.; Meinwald, Y. C.; Freed, J. H.; Scheraga, H. *J. Am. Chem. Soc.* **1981**, *103*, 7707.